Fibre optical temperature sensor for potential gas turbine applications

R D Pechstedt, A Sposito, C Langton

Oxsensis Ltd,
Rutherford Appleton Laboratory, Harwell Science and Innovation Campus,
Didcot, Oxfordshire, OX11 0QX,
ralf.pechstedt@oxsensis.com

Keywords: Optical temperature sensor, gas turbine

Abstract

In this paper we report on progress towards the development of a fibre optical temperature sensor suitable for long-term operation at temperatures above 1000°C. Basic design and working principles are reviewed. The sensor employs a sensing element made from single crystal sapphire capable of withstanding high temperatures without deterioration or structural change. Temperature measurement is facilitated by a readout unit that processes the reflected spectrum and yields the optical thickness of the sapphire sensing element as a function of temperature. First prototypes have been assembled and calibrated and are currently undergoing extended testing in a high-temperature furnace. Preliminary results indicate a temperature stability of ±1°C at 1100°C over a 40 day period. A resolution of better than 0.5°C was demonstrated without averaging. Achievable accuracy is estimated to be better than ±1.5°C, measured in the range between 700°C and 1300°C.

1 Introduction

Accurate knowledge of the temperature distribution in the hot zones of gas turbines are of increasing interest for optimizing design and operation of modern gas turbines. The direct combustor temperature measurement is a good example, but it is beyond the capability and reliability of most thermocouples due to the extreme temperatures present in the combustor. Instead, often the temperature distribution between the combustor cans is inferred from measurements of the exhaust gas temperature measurements at lower temperatures [1]. This however creates uncertainties regarding which combustor can is responsible for the temperature variation due to the possible angular shift of the temperature profile as the gas travels down the engine. Of further concern is the drift behaviour of thermocouples at higher temperatures. For instance, mineral insulated metal sheathed K and N type thermocouples can exhibit significant drift errors when operated above 1000°C, depending on temperature, geometrical dimensions and duration of exposure [2]. Although fibre optical temperature sensors based on Fibre Bragg Gratings in silica fibre have been demonstrated up to 1000°C, long-term stability is thought to be limited to around 800°C due to the start of softening of fused silica at about 850°C [3].

2 Design and Operating principle

The optical sensing element is formed by a thin slab of single crystal sapphire that is creating a simple Fabry-Perot (FP) cavity, a schematic of which is shown in Figure 1.

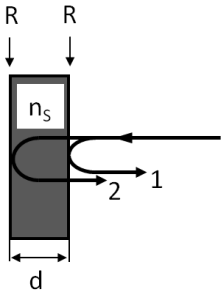

Fig.1: Schematic of Fabry-Perot cavity

Sapphire is a particularly attractive material for this application as it has a high melting point exceeding 2000°C. It is also highly transparent over a large wavelength range and its optical and mechanical properties are expected to remain highly stable at elevated temperature and over extended timescales due to its single crystal structure.

Optically, the sensor works as follows. An incoming light beam is partially reflected at the air-sapphire interface creating a first return beam 1. The non-reflected part of the beam is transmitted and then reflected at the sapphire-air interface, creating a second return beam 2 after having traversed the sapphire slab twice. Fresnel reflection at the air-sapphire interface is facilitated by the step change in refractive index n. For a planar wave the power reflectivity R can be calculated as

$$R = \frac{(n_S - 1)^2}{(n_S + 1)^2}, \qquad (1)$$

where n_S denotes the refractive index of sapphire and 1.0 is the refractive index of air. With n_S = 1.75 at a wavelength of 1550nm it is estimated that about 7% of incoming light is reflected. Whilst metal or dielectric coatings could be used to significantly increase the reflectivity, the pure Fresnel reflection is sufficient to generate a strong return signal. In addition, it very much simplifies the design as creating a high quality optical coating with reliable adhesion properties over

a 1000°C temperature range would represent a significant engineering challenge.

For practical application in a high-temperature environment the sapphire slab is mounted at the front end of an alumina tube and is illuminated by a beam of collimated light. The collimated beam is generated by a lens fixed in front of an optical fibre lead and both are attached to the rear end of the tube. The coefficients of thermal expansion of alumina and sapphire are closely matched, minimising thermal stresses at the interface between both materials. A sufficiently long tube therefore enables the front end to be exposed to very high temperatures whilst maintaining much lower temperatures that are compatible with silica fibre at the lensed end [4].

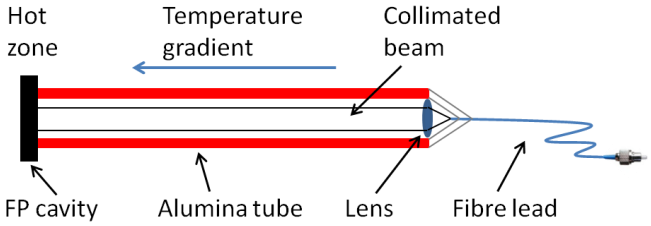

Fig.2: Schematic of temperature sensor

The first prototypes built employed an alumina tube of 20 cm lengths and 4mm diameter together with a sapphire slab of ~100um thickness.

On return beams 1 and 2 interfere and, because beam 2 travels the additional distance 2d, a phase delay of ϕ is generated between them:

$$\phi = \frac{4\pi n_S d}{\lambda} + \pi, \qquad (2)$$

where λ denotes the wavelength of the incoming light in vacuum and d is the thickness of the sapphire slab. The additional constant phase shift of π is generated at the reflection from the optically thinner (air) to thicker (sapphire) interface. Depending on the total phase shift ϕ, constructive (ϕ = even multiples of π) or destructive (ϕ = odd multiples of π) interference is observed, leading to a sinusoidal intensity pattern as a function of wavelength:

$$I = 1 - \cos\left(\frac{4\pi n_S d}{\lambda}\right). \qquad (3)$$

When illuminating the sapphire slab with a broadband light source containing a continuous multitude of wavelengths, the reflected light consists of a periodic fringe pattern of peaks and troughs in the wavelength domain. Figure 3 shows a schematic of the optical set-up used for this measurement. A super luminescent diode (SLD) with a centre wavelength around 1550nm is employed as a light source. It is emitting light over a broad wavelength range, typically between 50nm and 80nm. The light is then transmitted through an optical circulator and further to the optical sensor. The return light is travelling back via the same fibre lead and the circulator re-directs it to an optical spectrum analyser (OSA) that records optical power as a function of wavelength.

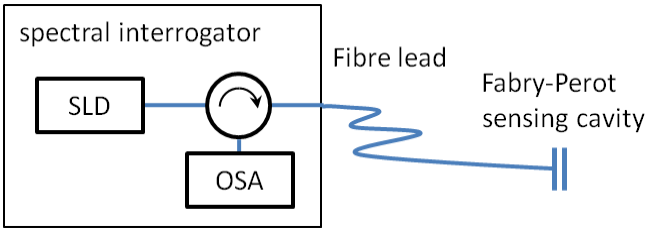

Fig.3: Schematic of optical set-up

An example of a measured return spectrum for the assembled prototype temperature sensor at 30°C is shown in Figure 4. The observed spectrum has a good modulation depth and the peaks and troughs are clearly identifiable. The Gaussian envelope replicates the spectral power distribution of the SLD. Changing either n_S or d or both modifies the conditions of constructive or destructive interference, resulting in a change of the positions of the peaks and troughs in the wavelength domain. Tracking the shift of a single peak allows *tracking changes in the optical thickness* $\Delta(n_S d)$. In addition, the distance between consecutive peaks is also changing slightly, and this information can be used to extract the *absolute value of the optical thickness* ($n_S d$):

$$n_S d = \frac{1}{2}\frac{\lambda_k \cdot \lambda_{k-1}}{\lambda_k - \lambda_{k-1}}, \qquad (4)$$

where λ_k and λ_{k-1} denote the wavelengths of two consecutive peaks. However, this calculation does not provide very accurate values for the optical thickness and in practice we employ a robust cross-correlation algorithm to extract the optical thickness to a very high degree of accuracy [5]. This approach calculates the cross-correlation between the measured return spectrum and a model spectrum of a single FP cavity. The main advantage of a spectral processing algorithm is that variations in optical power do not affect the position of the peaks or troughs in the wavelength domain, making the measurement result independent from environmental factors such as, for instance, vibration induced bend losses in the lead fibre. The superior modulation depth of the spectrum is maintained throughout and up to the maximum temperature range of 1300°C explored so far (see Figure 5).

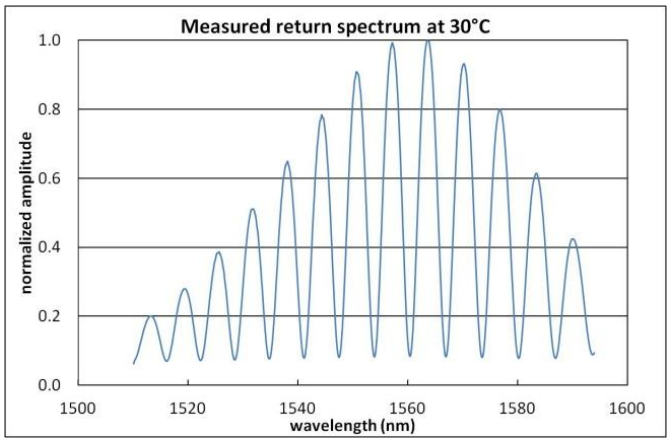

Fig.4: Measured return spectrum at 30°C

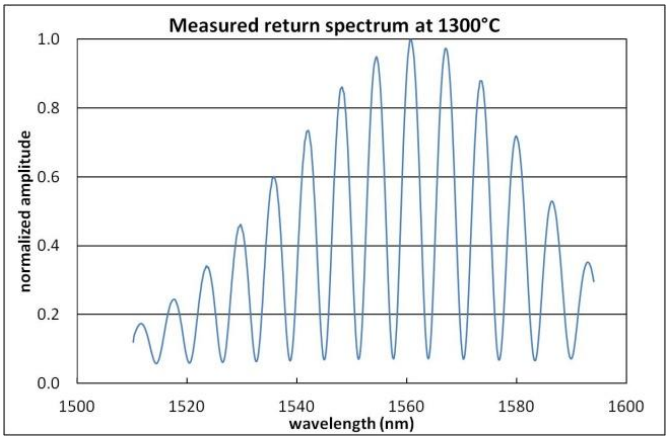

Fig.5: Measured return spectrum at 1300°C

The sensing mechanism for measuring temperature is based on the fact that both the refractive index n_S and the geometrical thickness d of the sapphire slab depend on temperature in a very consistent and repeatable way. The change in optical thickness $\Delta(n_S d)$ due to a change in temperature ΔT can be estimated as follows:

$$\Delta(n_S d) = d\left(\frac{dn_S}{dT} + n_S \alpha_S\right)\Delta T\,, \qquad (5)$$

where dn_S/dT denotes the thermo-optical coefficient and α_S is the coefficient of thermal expansion of sapphire. At room temperature dn_S/dT = $13\text{x}10^{-6}$/°C and α_S = $7.6\text{x}10^{-6}$/°C, leading to roughly equal contributions from both effects.

3 Measurement results

3.1 Initial temperature calibration

Initial measurements were carried out over a temperature range from room temperature up to 1100°C. The optical temperature sensor was placed in a Lenton UAF15/5 high-temperature furnace that is controlled via a PID feedback loop connected to an R-type embedded thermocouple located within the furnace. In addition, an N-type thermocouple was placed next to the optical sensor inside the furnace. Whilst both thermocouples read the same averaged temperatures, the N-type thermocouple exhibited a large noise that made its use as an accurate reference unsuitable. As a result of this the embedded R-type furnace thermocouple was used as a reference for all future measurements. We further observed that, with the standard factory-set PID values, the furnace temperature below 700°C was not stable but was oscillating due to repeatedly turning on and off the heating element. Accurate measurements were therefore limited in the first instance to temperatures above 700°C. The sensor was then calibrated by cycling the furnace temperature between 700°C and 1100°C in steps of 50°C, maintaining the temperature at each step for 5 hours. Average values of both furnace temperature and optical thickness were calculated at each temperature step during the first cycle to generate appropriate calibration points. Over the whole temperature range the optical thickness exhibits a non-linear dependence on temperature as shown in Figure 6. This is due to the fact that both the thermo-optical coefficient and the coefficient of thermal expansion of sapphire are not constant but also depend themselves on temperature. A polynomial curve fitting can be used to accurately describe the functional dependence, with residual values smaller than ±0.06°C between 700°C and 1100°C.

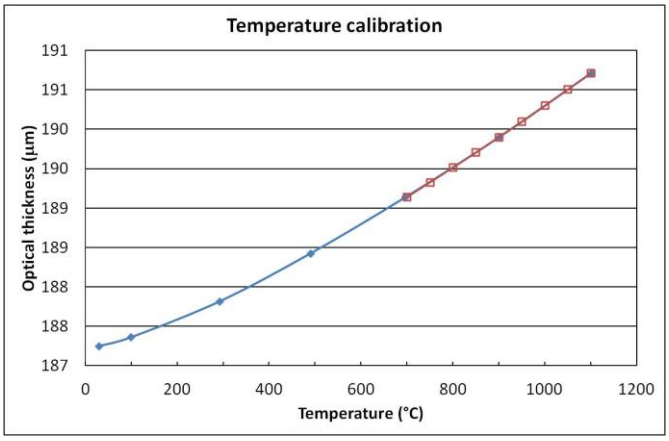

Fig.6: Optical thickness vs. temperature and calibration points (shown in red)

3.2 Stability test at 1100°C

The next test carried out was to evaluate the long-term stability of the optical sensor at elevated temperatures. For that the furnace was kept at a fixed temperature of 1100°C and outputs from both reference and optical sensors were recorded simultaneously. Figure 7 shows data sampled once per hour over ~ 1000 hours (~ 42 days). As can be seen, excellent stability of the optical sensor was observed, with a maximum variation of the optical sensor readings < ±1°C for the whole duration of the test.

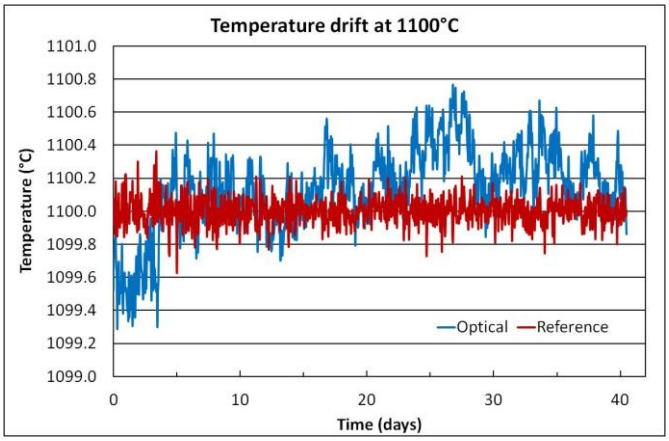

Fig.7: Stability test at 1100°C

3.3 Resolution test at 1100°C

In order to estimate the minimum detectable temperature variation of the optical sensor the furnace temperature was changed by 0.5°C at around 1100°C. Figure 8 shows the corresponding outputs from both the optical and reference

sensors, with data being recorded every 10 seconds. The graph confirms that a temperature step of 0.5C°C is clearly detectable. The test was then repeated with smaller steps and a running average of 30 points. Figure 9 shows an example of a 0.2°C step, from which it can be estimated that a resolution of ~0.1°C should be achievable. The reported measurements used a Labview based laboratory set-up that resulted in a relatively slow spectral capture and associated signal processing. Dedicated electronics could significantly increase the update rate of the sensor and ~kHz rates have been demonstrated internally using the spectral approach. For many applications this would enable to implement some form of running average to achieve a 0.1°C resolution whilst at the same time, maintaining a sufficiently high update rate.

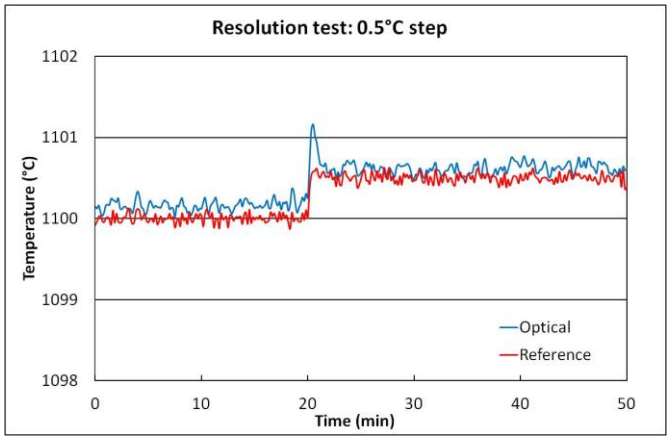

Fig.8: Resolution test using 0.5°C step

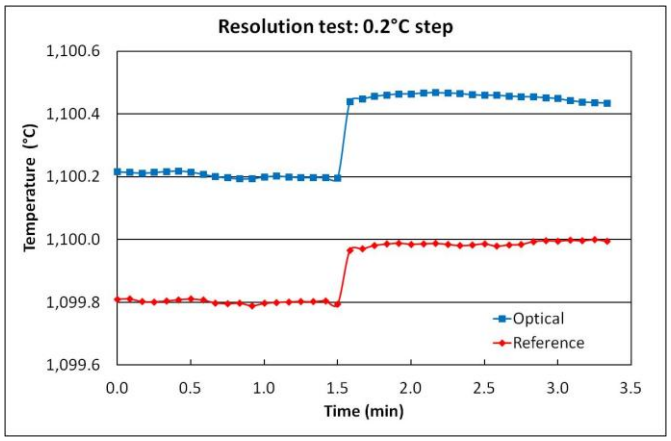

Fig.9: Resolution test using 0.2°C step (running average)

3.4 Calibration and accuracy test up to 1300°C

After the successful long-term stability test at 1100°C we decided to increase the upper working temperature to 1300°C. Initial calibration was carried out between 700°C and 1300°C in steps of 100°C in a similar fashion as before. A polynomial curve fitting with residual values less than ±0.15°C was used for generating the calibration curve. The sensor was then exposed to two complete temperature cycles between 700°C and 1300°C and the measurement error with respect to the reference sensor was calculated. Figure 10 show that the achieved accuracy of the optical sensor is ±1.5°C.

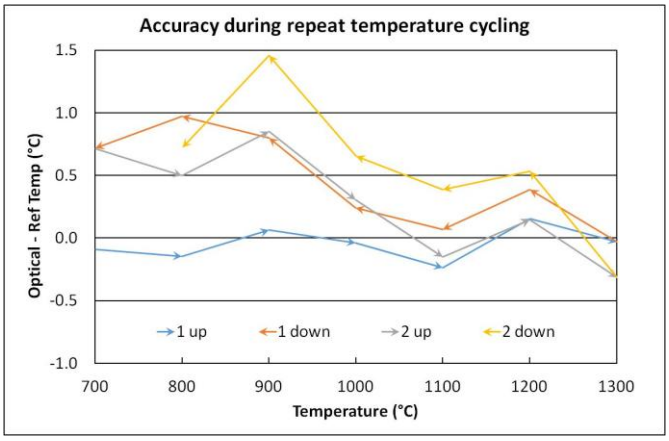

Fig.10: Measurement error during repeat temperature cycles

3.5 Stability test at 1300°C

A stability test at 1300°C was scheduled next and data from both the optical and reference sensors were recorded every hour and are plotted in Figure 11. As can be seen, after continuous exposure to 1300°C over the first 24 hours the optical sensor started to exhibit some limited drift downwards. The drift continued for the next 8.5 days, after which it reached a stable level about 1.5C lower than the reference sensor. Unfortunately, the furnace broke down after day 18 and testing had not re-started at the time of submitting the paper. The origin of limited drift observed is not known, but a burn-in at a higher temperature may be required to stabilize future sensor builds.

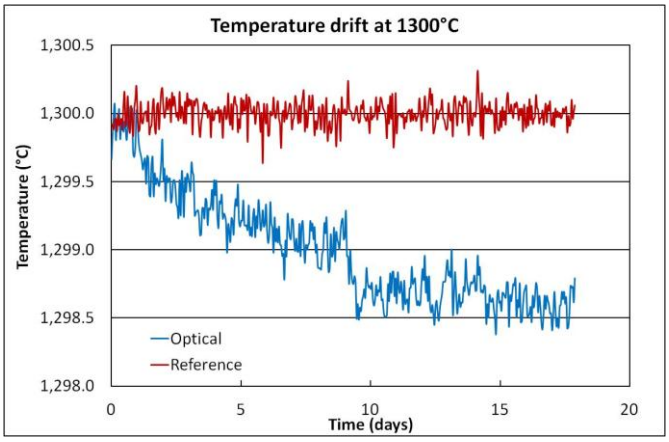

Fig.11: Stability test at 1300°C

4 Summary

First prototypes of a temperature sensor capable of operating long-term above 1000°C have been assembled and tested. The sensing element consists of a thin sapphire slab mounted at the front end of an alumina tube that is addressed by a collimated light beam propagating inside the tube. The tube itself is sufficiently long so that the front end can be exposed

to very high temperatures without damaging the rear end containing a lens and the silica based fibre lead. Initial measurements showed an excellent temperature stability of ±1°C at 1100°C over a 40 day period. At 1300°C, a limited drift of about 1.5°C was observed after which the sensor stabilized again during the remaining 9 days of the test. Without averaging, a resolution of better than 0.5°C was demonstrated at 1100°C. The achievable accuracy during repeated thermal cycling between 700°C and 1300°C is estimated to be better than ±1.5°C. The sensor could find promising applications for measuring temperature in the hot zones of gas turbines.

Acknowledgements

Support from the European Commission for funding the ASHLEY project during which the sensor was developed is gratefully acknowledged.

References

[1] A. Von Moll et al., "A Review of Exhaust Gas Temperature Sensing Techniques for Modern Turbine Engine Controls", 50th AIAA/ASME/SAE/ASEE Joint Propulsion Conference, Cleveland, OH, July 28-30, 2014.

[2] M. Scervini," Drift of nickel based mims thermocouples at temperatures above 1000°C: the effect of thermocouple diameter", XXI IMEKO World Congress "Measurement in Research and Industry" August 30 - September 4, (2015), Prague, Czech Republic.

[3] M. Willsch et al., "Design of Fiber Optical High Temperature Sensors for Gas Turbine Monitoring", Proc. SPIE, vol. 7503, p. 75037R, (2009).

[4] D.A. Jackson, "High temperature sensors exploiting low coherence signal recovery", Proc. SPIE, vol. 7004, p. 70040T, (2008).

[5] R.D. Pechstedt, "Fibre optic pressure and temperature sensor for applications in harsh environments", Proc. SPIE, vol. 8794, p. 879405, (2013).